

Monolithic Integration of GaN-Based Micromechanical Resonators and HEMTs for Timing Applications

Azadeh Ansari¹, Vikrant J. Gokhale¹, John Roberts², and Mina Rais-Zadeh¹

¹Department of Electrical Engineering & Computer Science, University of Michigan, Ann Arbor, MI 48109, USA

²Nitronex Corporation, Durham, NC 27703, USA

Phone: (734)764-4249, Fax: (734)763-9324, Email: azadans@umich.edu

Abstract

A platform for intimate integration of high-frequency gallium nitride (GaN) micromechanical resonators and AlGaN/GaN high electron mobility transistors (HEMTs) is reported. For the first time, cascade of a two-port GaN bulk acoustic resonator and AlGaN/GaN HEMT was co-fabricated on a silicon substrate. A high quality factor (Q) of 7413 is reported for a GaN contour-mode resonator at the resonance frequency of 119.8 MHz. More than 30 dB of signal tuning was achieved by using integrated HEMT for signal readout and amplification at the resonator output.

Introduction

Extensive research has been recently conducted on compound semiconductor materials, motivated by their superior material properties as compared to silicon. GaN, as a wide band-gap semi-conductor (3.4 eV) exhibits high saturation velocity, high breakdown electric field, and high sheet carrier density which make it applicable for high-frequency, high-power transistors. Also, its chemical and mechanical stability even at elevated temperatures along with excellent mechanical and piezoelectric properties make it a perfect candidate for sensing and timing applications in micro-electromechanical systems (MEMS) [1]. Fully integrated with CMOS technology, piezoelectric MEMS resonators based on AlN have replaced traditionally used off-chip quartz crystals in oscillator circuits and have shown significant potential as frequency references. However, pushing transistor cutoff frequencies beyond that of Si, and developing systems operable at harsh environments require devices based on materials such as GaN, which can endure high-frequency, high-temperature, and high-power operation. Previously, GaN only [2] and GaN-on-silicon [3] MEMS resonators with very high Q s and high power handling capability have been demonstrated by our group. However, the co-integration of MEMS components with GaN electronics has not been addressed to date.

GaN electronics take advantage of a two dimensional electron gas (2DEG) sheet that is induced at the AlGaN/GaN interface due to spontaneous and piezoelectric polarization. The 2DEG offers high sheet carrier concentration and mobility, forming the conducting channel of AlGaN/GaN HEMTs without intentional doping. Integration of confined 2DEG with GaN-based mechanical components opens up a wide area of interesting applications for all-GaN integrated micro-systems. Particularly, the 2DEG sheet can be employed as the bottom

electrode replacing metallization on backside of GaN resonators [4], or can be used in HEMTs for field-effect transistor (FET)-based actuation and sensing [5] with reduced parasitic feed-through, which is a critical issue in MEMS resonators and filters especially at high frequencies [6], [7]. There are two possible platforms to leverage advantages of both GaN micromechanical resonators and HEMTs. In the first platform, a piezoelectric resonant-body transistor can be implemented, where 2DEG acts as the bottom electrode and is modulated by the acoustic wave launched through Schottky contacts (from a second gate or a piezo actuator) (Fig. 1). HEMTs, as strain sensors use the exact same principle of operation; i.e. applied strain changes 2DEG mobility and sheet carrier density and thus the drain current [4]. In this approach, tuning and amplification of electrical signal can be achieved by different DC biasing of V_{DS} and V_{GS} . Thickness resonance mode can be excited through optimized design of inter-digitated electrodes to modulate the 2DEG channel current. This approach is a subject of future research.

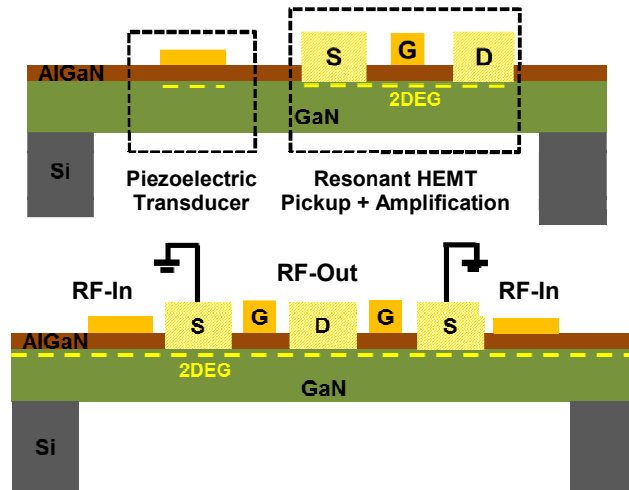


Fig. 1. Platform I (resonant-body HEMT): Confined 2DEG at AlGaN/GaN interface acts as the bottom electrode to actuate AlGaN layer piezoelectrically. (Top) Signal is actuated through a Schottky contact, then picked up and amplified by a resonant HEMT, (bottom) an example of a piezoelectric resonant-body transistor with two gates.

Platform II, which will be discussed in more detail in the following sections, incorporates piezoelectric actuation and sensing of GaN resonators, independent of HEMT (Fig. 2). The output of the resonator is fed to the gate of the HEMT, where the electrical signal gets picked up and amplified at the drain. This configuration has several advantages. First,

HEMT DC characteristics are set independent of the strain in the resonator; therefore, HEMT characteristics can be tightly controlled and as a result, any type of GaN-based circuitry can be fabricated. For instance, by simply connecting the GaN resonator input to the HEMT drain, a closed loop is formed, in which the resonance can be sustained with the addition of two capacitances connected to the gate and drain configuration) [8].

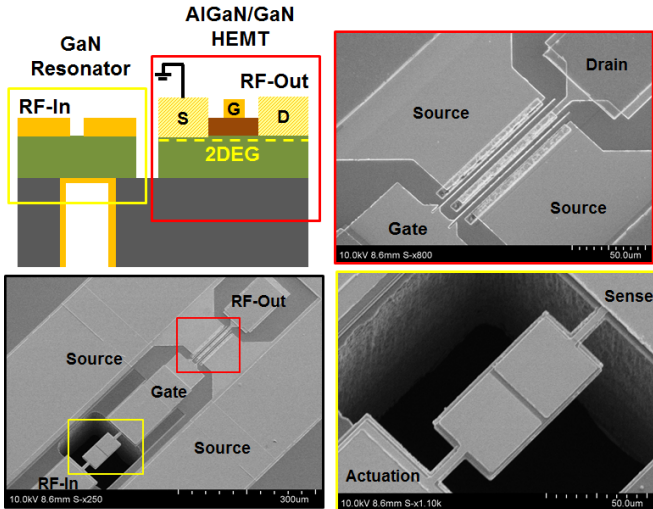


Fig. 2. An all-GaN integrated microsystem platform wherein GaN MEMS resonators are monolithically integrated with AlGaN/GaN HEMT. Resonator output is connected to the HEMT gate. SEM images of a GaN resonator co-fabricated with a two-gate AlGaN/GaN HEMT. Drain and source are 7 μm apart. Two-fingered gates are each 1 μm long and 100 μm wide. The resonator is a 40 $\mu\text{m} \times 80 \mu\text{m}$ contour-mode resonator.

Characterization and Fabrication

GaN is grown epitaxially on high-resistivity Si(111) substrate by metal-organic chemical vapor deposition (MOCVD). AlGaN/GaN HEMTs are traditionally fabricated on SiC or sapphire substrates. SiC is expensive, and sapphire suffers from low thermal conductivity, and thus high power limitation. GaN-on-Si takes advantage of the mature Si technology, which simplifies the resonator release. High quality wurtzite GaN can be grown epitaxially on Si(111) using an optimized nucleation layer. Here, the nucleation layer consists of 400 nm thick AlN and 650 nm thick AlGaN. GaN buffer layer (775 nm) is then grown followed by 175 Å of AlGaN barrier layer at nominal temperature of 1020 °C. 2DEG exists at about 20 nm below the sample surface, thus the surface is very sensitive to any electrical or chemical change and should be treated carefully. The fabrication of the HEMTs starts with mesa isolation; 2DEG is maintained at the mesa islands and removed elsewhere by BCl_3/Cl_2 plasma etch. Next, source and drain ohmic contacts are formed on the mesa islands. Ti/AI/Ti/Au multilayer is evaporated and lifted off, followed by 30 s of thermal annealing in N_2 environment at 900 °C to let the low-work function metal penetrate into the barrier layer and access the 2DEG channel with low resistance. The low resistance between ohmic contacts ensures higher current densities. Next, Ni/Au was used as Schottky contacts for gates and interconnect metallization.

Two-fingered HEMTs are fabricated, having gate length of 1 μm and width of 100 μm . Devices are then passivated with silicon nitride (Si_3N_4) using plasma enhanced chemical vapor deposition (PECVD) to improve RF performance and avoid current slump by reducing surface trapping effects [9]. Following the completion of HEMTs, GaN is plasma etched to create contours of the resonators, followed by top electrode (Ti/Au) deposition and lift-off. Openings are then created on Si_3N_4 film to allow interconnection of HEMTs and resonators with Ti/Au pads. Finally, devices are released from the backside using deep reactive ion etching (DRIE), and Ti/Au is sputtered on the back to serve as the bottom electrode of the resonators [10].

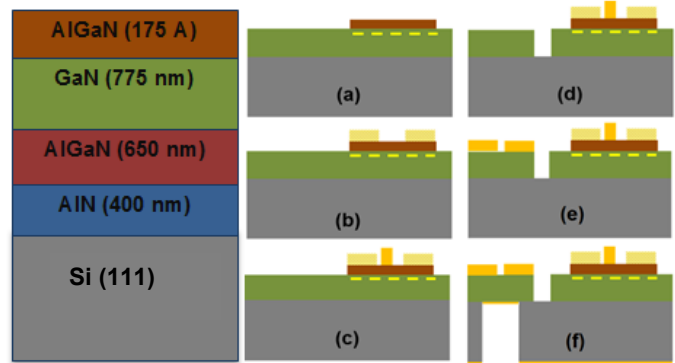


Fig. 3. (Left) AlGaN/GaN-on-Si epitaxial stack; 2DEG exists at the top AlGaN/GaN interface. (Right) Fabrication process flow; a) mesa isolation, b) drain and source ohmic contact formation, c) formation of gate Schottky contact, d) GaN plasma etch for resonator contours, e) resonator top electrode deposition, f) backside etch and gold back electrode deposition (right).

Device Operation

The integration scheme shown in Fig. 2 incorporates piezoelectric actuation and sensing of GaN resonators. The output of the resonator is connected to the gate of the HEMT, where the signal gets amplified by the HEMT intrinsic gain ($g_m \times Z_0$), tuned by different DC biasing of V_{DS} and V_{GS} , and finally gets collected from the drain of the HEMT.

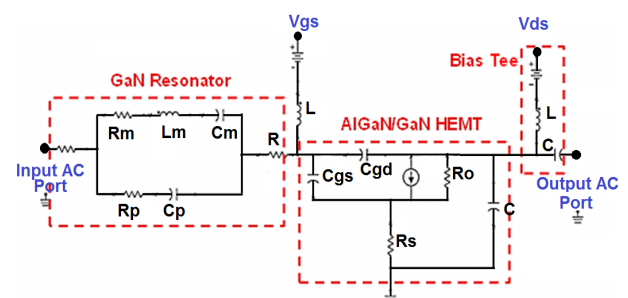


Fig. 4. Equivalent circuit model of the MEMS resonator cascaded with a HEMT. The output port of the resonator is connected to the gate of the HEMT, where the signal gets amplified and collected at the drain. The inductances connected to the gate and the drain model the Bias Tees.

The spontaneous and piezoelectric polarization due to lattice mismatch between AlGaN and GaN creates positive sheet charges in AlGaN at the hetero-interface. Due to the positive sheet charges, electrons appear and remain confined in the

potential well forming the 2DEG. In AlGaN/GaN HEMTs, the 2DEG conduction channel exists even with zero gate bias (depletion-mode transistor). The concentration of the 2DEG can be modulated by varying the voltage applied at the gate; thus, a negative DC voltage is applied to the gate of the transistor to ensure current is confined to the 2DEG channel and the AlGaN barrier layer does not get degraded [11].

Measurement Results and Discussion

RF measurements were carried out using a Lakeshore TTPX probe station, an Agilent N5241A PNA, and GSG ACP40 probes from Cascade Microtech. Short-Open-Load-Through (SOLT) calibration was performed prior to measurements. DC output characteristics of the HEMTs were measured using Keithly 4200-SCS parametric analyzer at operation temperature range of 100 K to 350 K. All measurements were taken with $50\ \Omega$ termination impedances.

GaN micromechanical resonators demonstrate very high $freq \times Q$ values, which make them desirable RF resonator blocks for timing and sensing applications [12]. Fig. 5 shows the frequency response of a two-port contour-mode GaN resonator. The Q is 7413 at room temperature and ambient pressure. In Fig. 6, the measured frequency and Q are shown at a temperature range of 100 K to 300 K. Temperature coefficient of frequency (TCF) is estimated to be -17.2 ppm/K at 300 K.

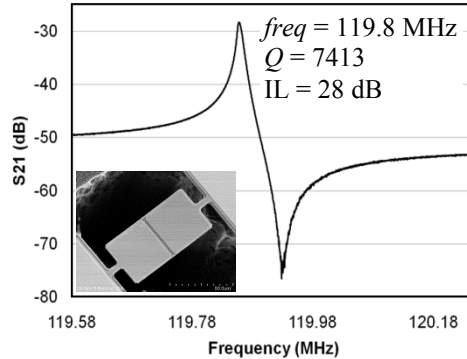


Fig. 5. Room temperature frequency response of a $40\ \mu\text{m} \times 80\ \mu\text{m}$ GaN resonator with center frequency (*freq*) of 119.8 MHz and high Q of 7413. This resonator exhibits the highest $freq \times Q$ amongst reported GaN resonators at room temperature.

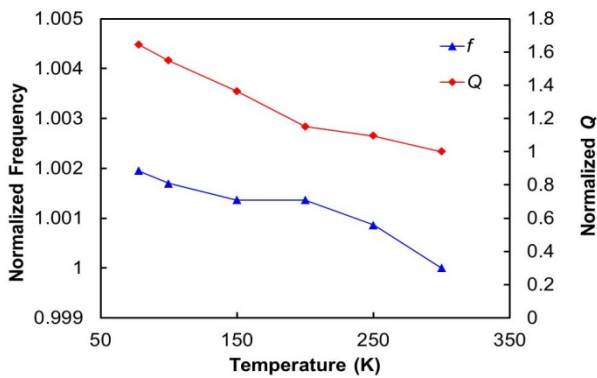


Fig. 6. Normalized resonance *freq* and measured Q of the GaN resonator depicted in Fig. 5 vs. temperature. TCF is calculated to be -17.2 ppm/K at 300 K.

Static I-V curves of a typical two-fingered HEMT with gate length of 1 μm and periphery of $2 \times 100\ \mu\text{m}$ are demonstrated in Figs. 7 and 8 at different temperatures. DC characteristics of HEMTs degrade slightly with increase in temperature due to an increase in the channel resistance. Unlike Si, AlGaN/GaN HEMTs have been reported to operate at elevated temperatures as high as 600 K [13]. Since the channel is formed without any intentional doping and a physical separation exists between parent atoms and the charges that form the 2DEG channel, temperature variations affect the 2DEG sheet carrier density only very slightly [14].

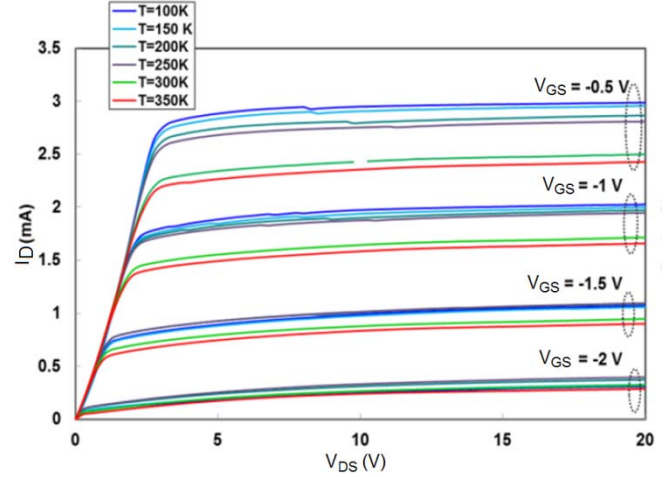


Fig. 7. DC I-V curves of a two-fingered, $100\ \mu\text{m}$ wide AlGaN/GaN HEMT. Drain current is plotted vs. drain-source voltage, with V_{GS} swept from -0.5 V to -2 V in -0.5 V steps. Low knee voltage of about 3 V is achieved, where the slope is proportional to 2DEG mobility, sheet carrier density, and device periphery. Temperature is varied from 100 K to 350 K. As expected, DC current decreases with increasing temperature.

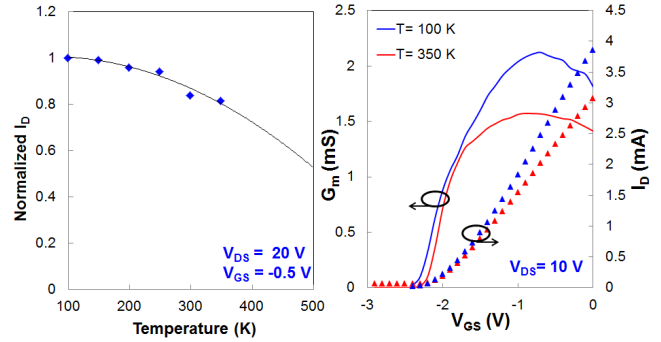


Fig. 8. (Left) Normalized drain DC current variation over temperature range of 100 K to 350 K with respect to its value at 100 K. The drain current is measured at $V_{GS} = -0.5\ \text{V}$ and $V_{DS} = 20\ \text{V}$. GaN HEMTs are expected to operate at temperatures up to 600 K; 350 K operation reported here is the measurement tool limit. (Right) Drain current and extrinsic transconductance vs. V_{GS} at 100 K and 350 K for $V_{DS} = 10\ \text{V}$. Both drain DC current and gain decrease relatively slightly with an increase in the temperature.

The large parasitic feed-through capacitance in the piezoelectric resonator is de-embedded from the response, using the method discussed in [15] where test devices with the same geometry as the resonators were laid out and fabricated, but only were not released from the back side. The test structures were used to de-embed the parasitic feed-

through capacitance created by interconnections and pads. Subtracting the two-port frequency response of the test structures from the total response results in a resonance peak due merely to the resonator piezoelectric response (Fig. 9).

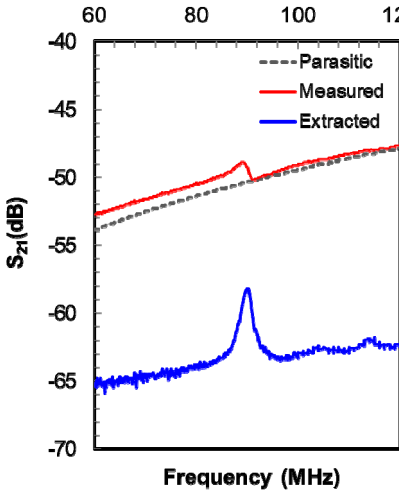


Fig. 9. Measured S_{21} response of a contour-mode resonator (red). A similar device is fabricated but not released to model parasitic feed-through capacitance (grey). Using a differential measurement setup or equivalently, subtracting the actual and parasitic 2-port frequency response results in de-embedded resonance peak (blue).

In Fig. 10, the frequency response of an integrated GaN resonator and HEMT (as shown in Fig. 2) is depicted. More than 30 dB of signal tuning is achieved using a HEMT biased at different DC levels. As shown below, peak values increase from ~ -56 dB for standalone resonator response to ~ -26 dB when HEMT is used at the resonator output and biased at $V_{DS} = 10$ V and $V_{GS} = -0.6$ V. Further amplification can be achieved with a proper output matching network, a lower loss resonator, and an optimized HEMT design. Ultimately, positive values of S_{21} can be reached, corresponding to negative net resistance values, which can be exploited in designing oscillators.

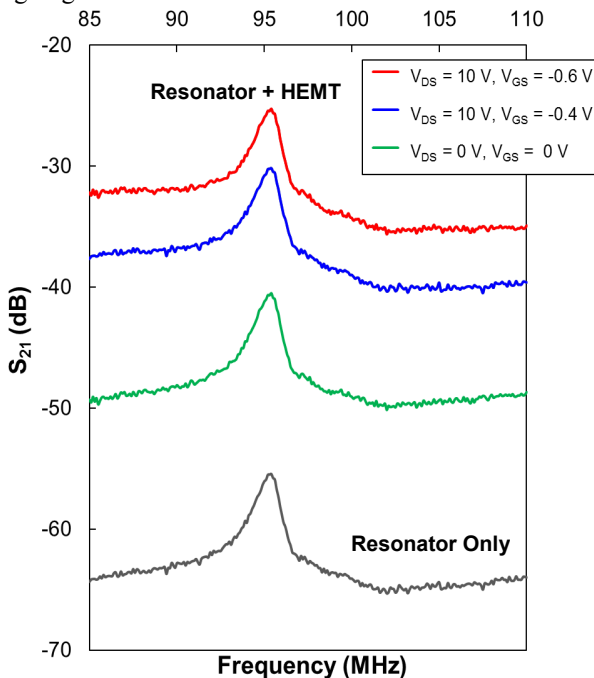


Fig. 10. S_{21} response of an integrated resonator + HEMT device shown in Fig. 2. With the proposed configuration, insertion loss level can be easily modulated using different gate biasing of the HEMT.

Conclusion & Future Work

In this work, for the first time, a platform for monolithic integration of GaN MEMS and GaN circuitry was proposed. As a proof of concept, a cascade of bulk acoustic mode GaN resonators and AlGaN/GaN HEMTs was successfully co-fabricated and a signal tuning of more than 30 dB was shown using the HEMT amplifier. GaN resonators with high Q s were also demonstrated. This work can be a starting point for further development of integrated GaN systems, where a combination of GaN-based devices (MEMS, HEMTs, resonant body HEMTs, etc.) can be all integrated to build different architectures such as all-GaN MEMS resonator-based oscillators or frequency references.

Acknowledgement

Fabrication of the devices was carried out at Lurie Nanofabrication Facility at the University of Michigan. This work was funded by the U.S. Army Research Laboratory under contract W911NF and prepared through collaborative participation in the MAST CTA and by NSF under award # 1002036.

References

- [1] V. Cimalla, J. Pezoldt, and O. Ambacher, "Group III nitride and SiC based MEMS and NEMS: materials properties, technology and applications," *J. Phys. D, Appl. Phys.* 40, 6386–6434, 2007.
- [2] V. J. Gokhale, J. Roberts, and M. Rais-Zadeh, "High-performance bulk-mode gallium nitride resonators and filters," *Transducers'11*, Beijing, China, June 2011.
- [3] A. Ansari, et al., "Gallium nitride-on-silicon micromechanical overtone resonators and filters," *IEDM'11*, pp. 485–488, Washington, DC, Dec 2011.
- [4] Niebelshutz et al., "AlGaN/GaN-based MEMS with two-dimensional electron gas for novel sensor applications," *phys. stat. sol. (c)* 5, No. 6, 1914–1916, 2008.
- [5] M. Faucher et al., "Electromechanical transconductance properties of a GaN MEMS resonator with fully integrated HEMT transducers," *JMEMS*, Vol. 21, No. 2, April 2012.
- [6] E. Hwang, A. Driscoll and S. A. Bhave, "Platform for JFET-based sensing of RF MEMS resonators in CMOS technology," *IEDM '11*, pp. 489–492. Washington, DC, Dec 2011.
- [7] D. Weinstein, S. A. Bhave, "The resonant body transistor," *Nano Lett.* 10(4) 1234–37, 2010.
- [8] V. S. Kaper et al., "High power GaN Monolithic AlGaN/GaN oscillator," *IEEE JSSC*, Vol. 38, No. 9, Sept. 2003.
- [9] B. M. Green et al., "The effect of surface passivation on the microwave characteristics of undoped AlGaN/GaN HEMT's," *IEEE Electron Device Lett.*, Vol. 21, No. 6, June 2000.
- [10] L. F. Eastman et al., "Undoped AlGaN/GaN HEMTs for microwave power applications," *IEEE Transaction on Electron Devices*, Vol. 48, No. 3, March 2001
- [11] D. Ducatteau et al., "Output power density of 5.1/mm at 18 GHz with an AlGaN/GaN HEMT on Si substrate," *IEEE Electron Device Lett.*, Vol. 27, No. 1, Jan. 2006.
- [12] V. J. Gokhale, Y. Sui, and M. Rais-Zadeh, "Novel uncooled detector based on gallium nitride micromechanical resonators," *Proc. SPIE 8353, Infrared Technology and Applications XXXVIII*, May 2012.
- [13] N. Adachi et al., "High temperature operation of AlGaN/GaN HEMTs," *IEEE MTT-S*, pp. 507–510, 2005.
- [14] M. A. Haque et al., "Temperature dependent analytical model for current-voltage characteristics of AlGaN/GaN power HEMT," *Solid-State Electronics*, Vol. 53, pp. 341–348, 2009.
- [15] K. E. Wojciechowski, "Single-chip precision oscillators based on multi-frequency, high- Q aluminum nitride MEMS resonators," *Transducers'09*, Denver, June 2009.